Effect of Fluorine Substitution on the Aromaticity of Polycyclic Hydrocarbons

ARTICLE *in* THE JOURNAL OF PHYSICAL CHEMISTRY A · SEPTEMBER 2012

Impact Factor: 2.69 · DOI: 10.1021/jp308121b · Source: PubMed

5 AUTHORS, INCLUDING:

Mikko Kaipio
University of Helsinki
4 PUBLICATIONS **16** CITATIONS
SEE PROFILE

Michael Patzschke
University of Helsinki
27 PUBLICATIONS **578** CITATIONS
SEE PROFILE

Heike Fliegl
University of Oslo
36 PUBLICATIONS **851** CITATIONS
SEE PROFILE

Dage Sundholm
University of Helsinki
205 PUBLICATIONS **4,623** CITATIONS
SEE PROFILE

THE JOURNAL OF PHYSICAL CHEMISTRY A

Article

pubs.acs.org/JPCA

Effect of Fluorine Substitution on the Aromaticity of Polycyclic Hydrocarbons

Mikko Kaipio,*[,†] Michael Patzschke,*[,†] Heike Fliegl,*[,‡] Fabio Pichierri,*[,§] and Dage Sundholm*[,†]

[†]Department of Chemistry, University of Helsinki, P.O. Box 55 (A.I. Virtanens plats 1), FIN-00014 Helsinki, Finland

[‡]Centre for Theoretical and Computational Chemistry (CTCC), Department of Chemistry, University of Oslo, P.O. Box 1033 Blindern, 0315 Oslo, Norway

[§]Department of Applied Chemistry, Graduate School of Engineering, Tohoku University, Aoba-yama 6-6-07, Sendai 980-8579, Japan

Supporting Information

ABSTRACT: The effect of fluorine substitution on the aromaticity of polycyclic hydrocarbons (PAH) is investigated. Magnetically induced current densities, current pathways, and current strengths, which can be used to assess molecular aromaticity, are calculated using the gauge-including magnetically induced current method (GIMIC). The degree of aromaticity of the individual rings is compared to those obtained using calculated nucleus-independent chemical shifts at the ring centers (NICS(0) and NICS(0)$_{zz}$). Calculations of explicitly integrated current strengths for selected bonds show that the aromatic character of the investigated polycyclic hydrocarbons is weakened upon fluorination. In contrast, the NICS(0) values for the fluorinated benzenes increase noteworthy upon fluorination, predicting a strong strengthening of the aromatic character of the arene rings. The integrated current strengths also yield explicit current pathways for the studied molecules. The current pathways of the investigated linear polyacenes, pyrene, anthanthrene, coronene, ovalene, and phenanthro-ovalene are not significantly affected by fluorination. NISC(0) and NICS(0)$_{zz}$ calculations provide contradictory degrees of aromaticity of the fused individual ring. Obtained NICS values do not correlate with the current strengths circling around the individual rings.

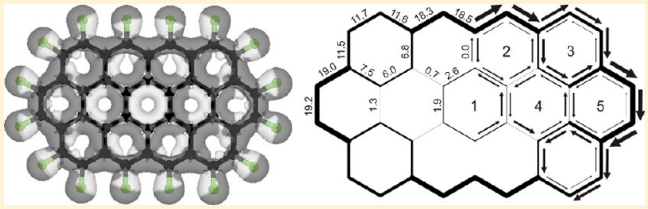

1. INTRODUCTION

Fluorine is well known for having the highest electronegativity of 3.98 (on the Pauling scale) among those assigned to the elements of the periodic table.[1] Electronegativity, which represents the relative tendency of an element to withdraw electrons when bonded to different elements, has been shown to correlate with electronic, structural, and spectroscopic properties of molecules.[2−5] Structural effects arising from fluorine substitution were already noticed and rationalized by Bent in the 1960s.[2] According to Bent's rule, electronegative substituents bonded to carbon display smaller bond angles with respect to substituents of low electronegativity as a result of the increased p character of the corresponding sp hybrid orbital of the carbon atom. Structural distortions that arise with β-fluorine substitution in porphyrins have been reported by Bondon et al.,[6] who discovered interesting correlations between the position of the Soret band and the averaged chemical shifts of the NH protons with respect to the number of fluorine atoms in both neutral and diprotonated porphyrins. The shifts in the ultraviolet absorption spectra at the Soret band and changes in the NH nuclear magnetic resonance (^{1}H NMR) chemical shifts suggest that the aromatic properties of porphyrins are altered by fluorine substitution. Spectroscopic studies showed that perfluorination increases the resistance toward oxidation in platinum porphyrin.[7]

Fluorination also plays an important role in bio-organic chemistry and medicinal chemistry.[8,9] Liu et al., for example, synthesized a perfluorinated manganese corrolate complex, which displayed very good reactivity and stability in the catalytic oxidation of alkenes.[10] On the other hand, fluorinated compounds are dangerous to the environment and must constantly be monitored.[11] The electronic structure of polyaromatic hydrocarbons can also be adjusted by fluorination. A recent theoretical study of perfluorinated hydrocarbons such as perfluoroanthracene, perfluorotetracene, and perfluorophenanthrene showed that these types of molecules are very effective electron acceptors. It was suggested that perfluorinated benzenoid compounds could be used as starting materials for manufacturing stable novel magnetic materials.[12] Perfluorination of pentacene and partial fluorination of hexaperi-hexabenzocoronene has recently been exploited to convert p-type organic semiconductors into n-type ones.[13,14] A number of theoretical studies indicate that fluorination affects the strength of intra- and

Received: August 15, 2012
Revised: September 12, 2012
Published: September 20, 2012

Table 1. Comparison of Current Strengths (in nA/T) with NICS(0) and NICS(0)$_{zz}$ Values (in ppm) Calculated for Benzene and Fluorinated Benzene Derivatives

molecule	total	diatropic	paratropic	NICS(0)	NICS(0)$_{zz}$
benzene	11.6	16.9	−5.3	−8.4	−12.1
monofluorobenzene	11.1	16.0	−5.0	−9.8	−7.6
1,2-difluorobenzene	10.6	14.8	−4.1	−11.3	−9.2
1,3-difluorobenzene	10.5	15.0	−4.6	−11.3	−11.7
1,4-difluorobenzene	10.4	15.3	−4.9	−11.1	−12.1
1,2,3-trifluorobenzene	10.1	14.3	−4.3	−12.6	−12.0
1,2,4-trifluorobenzene	10.0	13.9	−3.9	−12.7	−12.9
1,3,5-trifluorobenzene	9.7	14.0	−4.2	−12.4	−12.2
1,2,3,4-tetrafluorobenzene	9.7	13.7	−4.0	−14.0	−15.1
1,2,4,5-tetrafluorobenzene	9.6	13.1	−3.5	−14.1	−13.7
1,2,3,5-tetrafluorobenzene	9.5	13.3	−3.8	−13.8	−13.1
pentafluorobenzene	9.2	12.6	−3.4	−15.3	−17.1
hexafluorobenzene	9.0	11.9	−3.0	−16.5	−15.3

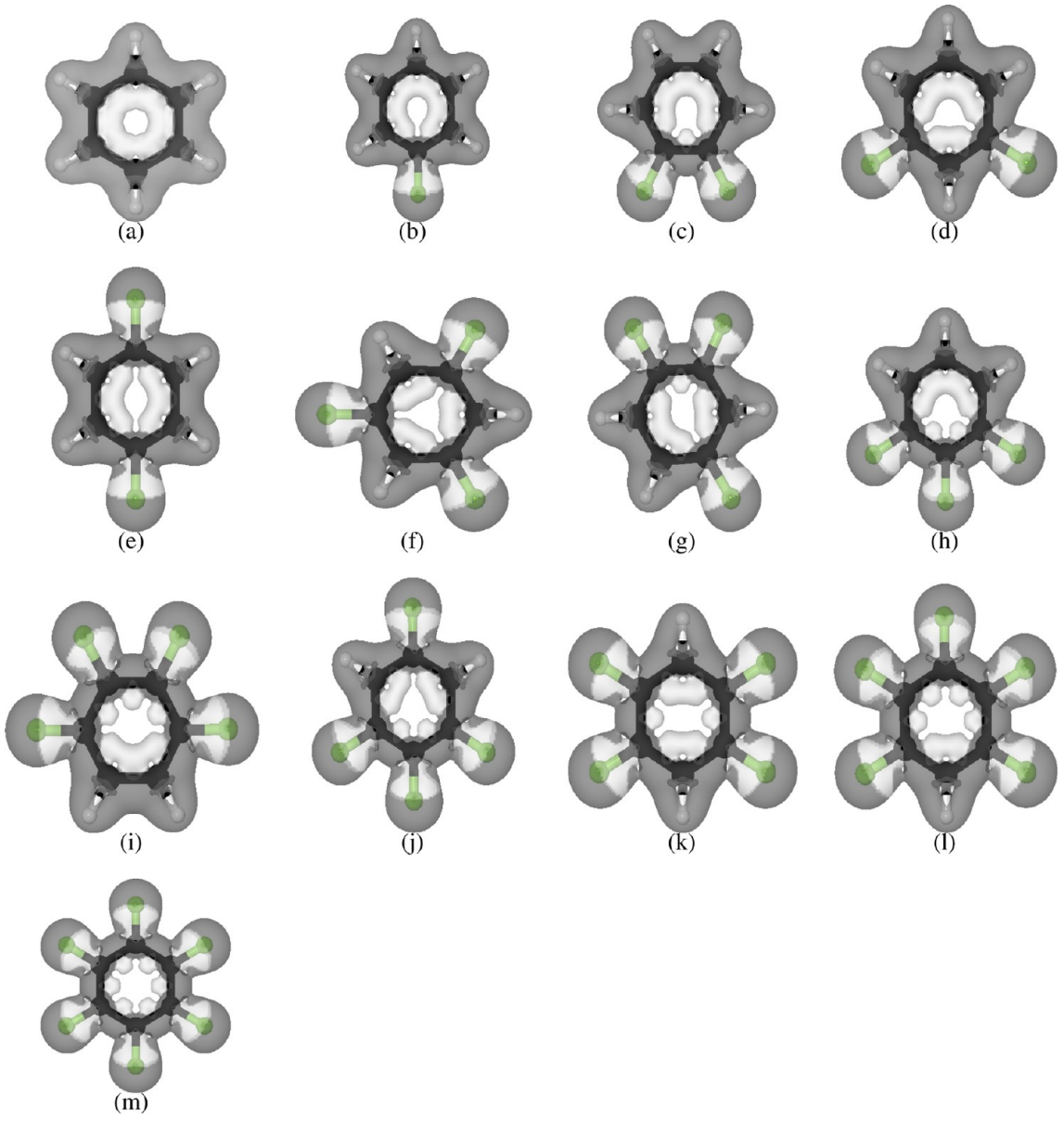

Figure 1. Signed modulus of the magnetically induced current densities calculated at the BP86/SVP level for (a) benzene, (b) monofluorobenzene, (c) 1,2-difluorobenzene, (d) 1,3-difluorobenzene, (e) 1,4-difluorobenzene, (f) 1,3,5-trifluorobenzene, (g) 1,2,4-trifluorobenzene, (h) 1,2,3-trifluorobenzene, (i) 1,2,3,4-tetrafluorobenzene, (j) 1,2,3,5-tetrafluorobenzene, (k) 1,2,4,5-tetrafluorobenzene, (l) pentafluorobenzene, and (m) hexafluorobenzene. Diatropic currents are gray, and paratropic ones are white.

dx.doi.org/10.1021/jp308121b | J. Phys. Chem. A 2012, 116, 10257−10268

intermolecular hydrogen bonds (H bonds)[15−17] as well as the inversion barrier in organic molecules such as bicyclo-[1.1.0]butane.[18] The electron-withdrawing property of substituted fluorines affects the electronic structure of conjugated molecules since fewer electrons are then available for electron delocalization. By using the same line of arguments, the weaker H bonds of fluorinated molecules as compared to the unsubstituted ones can also be understood. A recent computational study showed that the H-bond strengths of hydrogen-bonded systems are linearly related to the degree of electron delocalization across the H bond as obtained using the gauge-including magnetically induced current method (GIMIC).[19] Thus, the electron-withdrawing fluorine substituents decrease the amount of electrons that can contribute to the electron delocalization across H bonds.

The effect of perfluorination on the degree of aromaticity of arenes has been debated. While Okazaki and Laali concluded that fluorination leads to a decrease in the strength of the ring currents,[20] Wu et al. found that fluorination has no effect on the aromaticity of arene rings.[21] In both studies, the conclusions were based on the strengths of the magnetically induced ring currents estimated using various nucleus-independent chemical shift (NICS) calculations.[22] In this work, the effect of fluorination on electron delocalization and degree of aromaticity of fluorinated benzenes and perfluorinated polycyclic aromatic hydrocarbons is investigated by performing explicit calculations of magnetically induced current densities using the gimic method.[23,24] The aromatic properties are judged from the extent of electron delocalization and the pathways for electron transport in the conjugated molecules. Numerical integration of the magnetically induced current strengths (current susceptibilities) passing selected bonds has proven to be a reliable method to determine the degree of molecular aromaticity of single-ring organic[25] and inorganic molecules[26−29] to assess the aromaticity of the individual rings in polycyclic molecules.[30−38] The employed GIMIC method inclusive of applications has recently been reviewed in a perspective article.[39]

2. COMPUTATIONAL DETAILS

All molecular structures were optimized at the density functional theory (DFT) level using Turbomole.[40] The Becke−Lee−Yang−Parr three-parameter hybrid functional (B3LYP) was used with the Karlsruhe double-ζ (def2-SVP) basis set augmented with polarization functions.[41−44] Optimized structures were confirmed to be minima by evaluating structural force constants.[45] Nuclear magnetic shielding tensors were calculated with Turbomole at the DFT level using the Becke−Perdew (BP86) functional and def2-SVP basis set.[44,46−51] The quality of the calculated shieldings with respect to the employed basis set has been checked using triple-ζ (def2-TZVP) basis sets.[43] The prefix def2 is omitted in the following. Basis-set effects were investigated for benzene, which was chosen to represent the studied molecules. ^{1}H NMR shieldings calculated using the SVP and TZVP basis sets differ at most by 0.2 ppm (1%).

Ring-current susceptibilities yielding the ring-current strengths for a given value of the external magnetic field were calculated using GIMIC.[23,24,39] GIMIC is an independent program that uses basis-set information as well as the magnetically perturbed and unperturbed one-body density

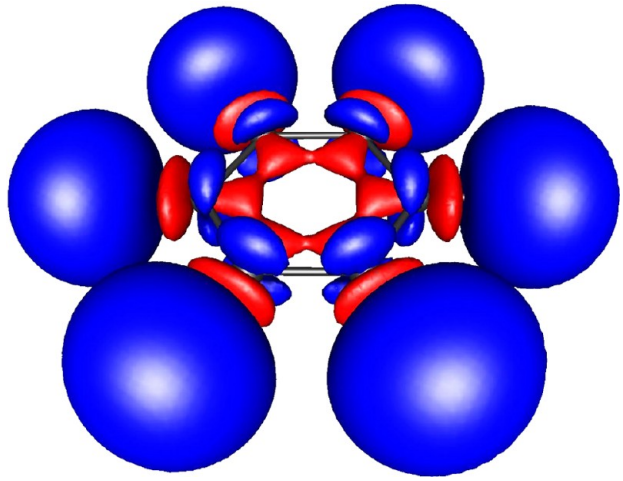

Figure 2. Plot of the electron-density difference between fluorinated benzene and benzene: (blue) increase in the electron density of the fluorinated species; (red) electron depletion. In the calculation, the positions of the carbon atoms were unchanged, whereas the fluorines were put at the optimized C−F distance. C−C bond lengths of benzene are only 0.24 pm longer than for perfluorinated benzene. Big blue spheres at the fluorine position arise from the electron density difference between fluorine and hydrogen. Plot was created with gOpenMol.[63,64]

matrices obtained in the NMR shielding calculations as input data.[23,24] The obtained current densities are origin independent with a fast basis-set convergence, because gauge-including atomic orbitals (GIAO) are used.[49,52−54] Explicit values for current strengths (susceptibilities) are obtained by numerical integration of the current density passing through cut planes perpendicularly to selected bonds of the molecular system.[23] The ring-current susceptibility at zero magnetic field, which we denote ring-current strength in the rest of this work, can be used as a reliable measure of molecular aromaticity.[39] The sign and magnitude of the obtained ring-current strengths indicate whether molecular rings are aromatic, antiaromatic, or nonaromatic, thus having diatropic, paratropic, or vanishing net ring current, respectively.[25] The signed modulus of the current densities drawn in the plots indicates where diatropic and paratropic currents dominate.

The net current strength for benzene calculated at the BP86/SVP level is 11.6 nA/T, which agrees well with the value of 11.8 nA/T previously obtained at the B3LYP/TZVP level.[25] For benzene, a change in the ring-current strength of 0.2 nA/T (2%) was obtained when increasing the basis set from SVP to TZVP. Thus, accurate current densities are obtained already when SVP quality basis sets are used. Integrated current strengths in combination with current-density plots provide detailed information about current pathways of hydrocarbon multiring systems and can be employed for assessing the aromaticity even for very complicated Möbius twisted molecules.[32,35,37,39] In this work current density plots are created with Jmol,[55] current-strength profiles are obtained using gnuplot[56] and gimp,[57] and current pathways are visualized using ChemDraw.[58]

Nucleus-independent chemical shifts at the ring centers were calculated at the BP86/SVP level. The negative value of the nuclear magnetic shielding in the ring center is denoted NICS(0).[59] We also report NICS$_{zz}$(0) values, which

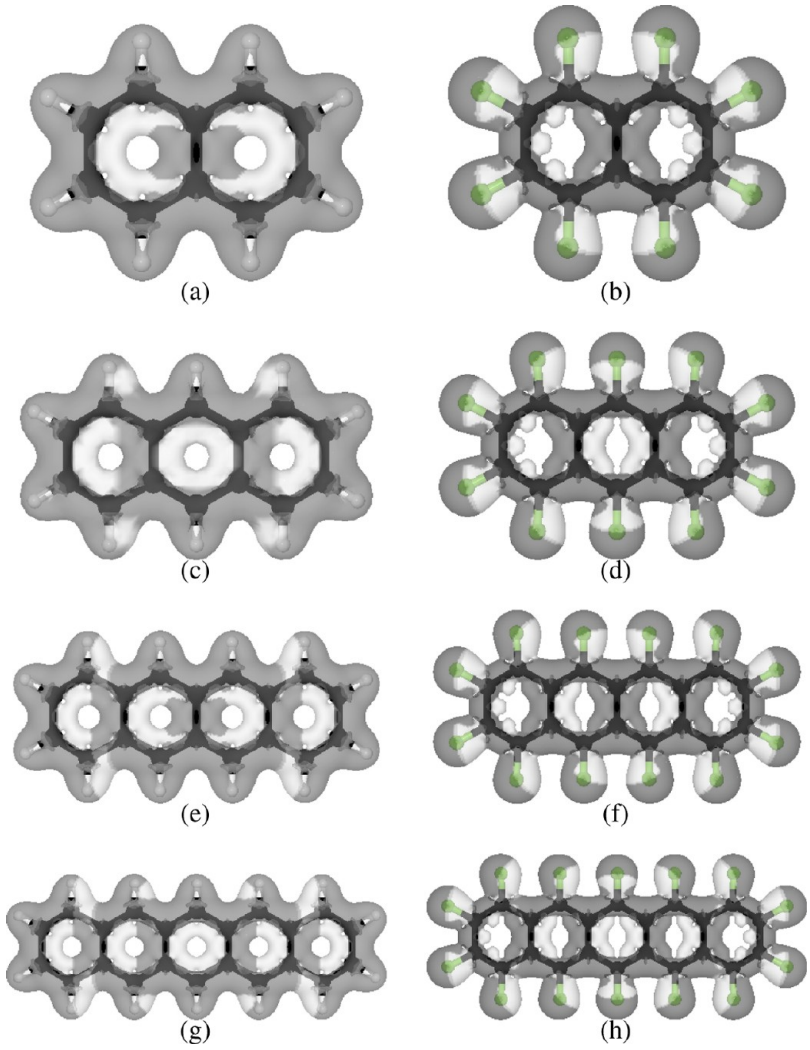

Figure 3. Signed modulus of the magnetically induced current densities calculated at the BP86/SVP level for (a) naphthalene, (b) perfluoronaphthalene, (c) anthracene, (d) perfluoroanthracene, (e) tetracene, (f) perfluorotetracene, (g) pentacene, and (h) perfluoropentacene. Diatropic currents are gray, and paratropic ones are white.

Table 2. Comparison of Current Strengths (in nA/T) with the NICS(0) and NICS(0)$_{zz}$ Values (in ppm) Calculated for the Linear Polyacenes and Perfluorinated Ones[a]

molecule	total	diatropic	paratropic	ring number	NICS(0)	NICS(0)$_{zz}$
naphthalene	12.7	17.6	−4.9	1	−8.7	−11.3
perfluoronaphthalene	10.4	13.1	−2.7	1	−15.1	−13.6
anthracene	15.6	20.2	−4.6	1	−11.1	−16.4
	12.1	17.1	−4.9	2	−7.7	−8.1
perfluoroanthracene	12.8	17.2	−4.4	1	−14.2	−14.9
	10.1	12.9	−2.7	2	−14.7	−11.8
tetracene	16.1	20.6	−4.5	1	−11.1	−16.4
	11.3	16.7	−5.4	2	−6.8	−5.3
perfluorotetracene	13.3	17.7	−4.4	1	−14.4	−15.3
	9.7	12.5	−2.8	2	−14.0	−9.8
pentacene	17.4	21.8	−4.3	1	−12.0	−18.9
	15.8	20.4	−4.6	2	−10.6	−14.8
	10.6	16.1	−5.5	3	−6.1	−3.1
perfluoropentacene	14.3	18.6	−4.3	1	−15.1	−17.2
	13.0	17.4	−4.4	2	−14.0	−14.1
	9.2	12.1	−2.9	3	−13.5	−8.1

[a]Ring labels and current strengths are also shown in Figure 4.

correspond to the zz element (z is perpendicular to the molecular plane) of the shielding tensor with opposite sign, since they have been suggested to better reflect the currents in planar π rings.[60,61]

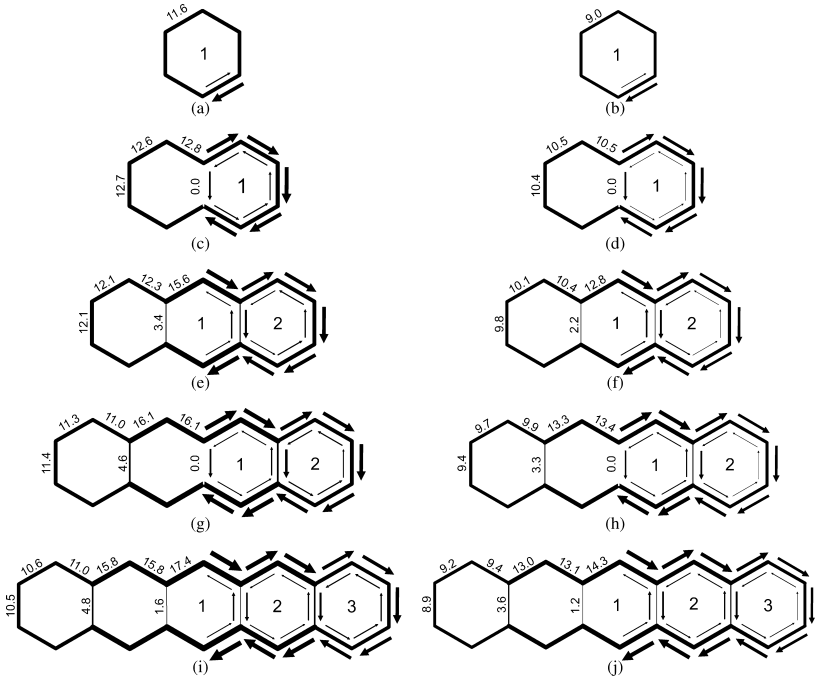

Figure 4. Integrated current strengths and current pathways for benzene, naphthalene, anthracene, tetracene, and pentacene (left) as well as their perfluorinated derivatives (right). Benzenoid rings are numbered taking the molecular symmetry into account.

3. RESULTS AND DISCUSSION

3.1. Benzenes. The integrated ring-current strengths for benzene and for the 12 possible fluorinated benzene derivatives are given in Table 1, where they are compared to NICS(0) and $NICS_{zz}(0)$ values. The signed modulus of the magnetically induced current densities, depicted in Figure 1, shows that fluorination decreases the diatropic ring current flowing along the outer edge of the molecular ring explaining the smaller ring-current strengths of the fluorinated derivatives as compared to the unsubstituted one. Benzene and the fluorinated benzenes have net diatropic current strengths ranging between 11.6 nA/T for benzene and 9.0 nA/T for hexafluorobenzene. Thus, according to the ring current criterion all fluorinated benzene derivatives are aromatic. The diatropic and paratropic contributions to the net ring-current strengths diminish with increasing degree of fluorination. Fluorination causes a deficit of electrons, which hampers the current flow in the σ orbitals (vide infra). Depletion of the σ electrons reduces the diatropic current contribution along the molecular edge as well as the paratropic one inside the ring. The small gaps in the paratropic current density inside the ring of the fluorinated benzenes indicate that the paratropic currents are mainly localized to the bonds instead of forming a continuous flow around the ring as in benzene, see Figure 1. The diatropic contribution decreases with almost 1 nA/T per fluorine atom, whereas the paratropic contribution decreases by roughly 0.5 nA/T per fluorine atom. Thus, the total current strength decreases approximately by 0.5 nA/T per substituted fluorine atom. The fluorine-substitution pattern seems to have little effect on the total current strengths, since the current strengths of the different isomers vary by only 0.1−0.4 nA/T. Thus, according to the current-density calculations, benzene is the most aromatic molecule as compared to the fluorinated benzene derivatives.

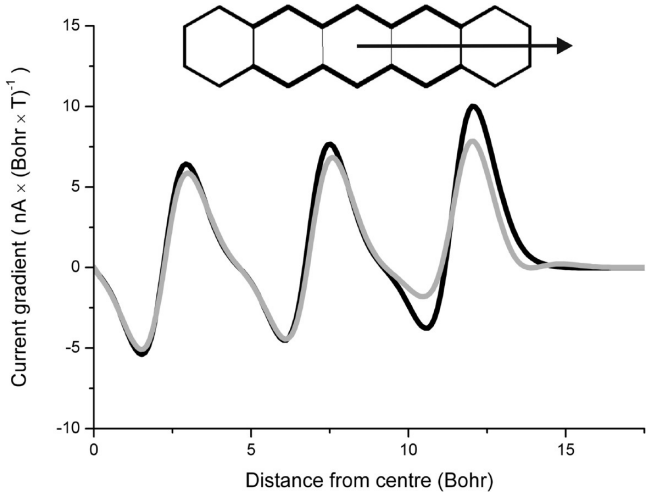

Figure 5. Integrated current strength as a function of the distance from the center of the molecule calculated for pentacene (black) and perfluoropentacene (gray). Plane of the current profile is indicated by the arrow.

The same argument can be used to explain the perfluoro effect of Brundle et al.[62] They dubbed the strong stabilization of σ orbitals compared to a weak stabilization of π orbitals in perfluorated systems, the so-called perfluoro effect. The explanation for this would be that σ electrons are moved to fluorine, which binds them stronger than carbon. This then deshields the nuclear charge of carbon, which somewhat lowers the π orbitals in energy. Their findings are in agreement with our assessment of the change in ring currents upon fluorination.

The NICS(0) and $NICS_{zz}(0)$ aromaticity indices also suggest that all investigated fluorinated benzene derivatives are aromatic. However, the NICS(0) values increase with increasing number of fluorine substituents from −8.4 ppm for

dx.doi.org/10.1021/jp308121b | J. Phys. Chem. A 2012, 116, 10257−10268

Table 3. Comparison of Current Strengths (in nA/T) with the NICS(0) and NICS(0)$_{zz}$ Values (in ppm) Calculated for Pyrene, Anthanthrene, and Coronene and the Perfluorinated Ones[a]

molecule	total	diatropic	paratropic	ring number	NICS(0)	NICS(0)$_{zz}$
pyrene	10.9	15.9	−5.1	1	−3.9	+5.1
	15.8	20.4	−4.6	2	−11.2	−17.5
perfluoropyrene	9.0	13.8	−4.8	1	−8.6	+2.7
	13.4	15.7	−2.4	2	−15.8	−18.0
anthanthrene	15.7	20.2	−4.5	1	−8.4	−7.1
	8.6	14.0	−5.4	2	−0.8	+14.7
	16.3	20.9	−4.6	3	−11.1	−17.1
perfluoroanthanthrene	13.5	17.6	−4.1	1	−10.7	−6.8
	7.4	12.6	−5.2	2	−5.8	+11.4
	14.1	16.4	−2.3	3	−15.9	−18.2
coronene	−5.0	6.4	−11.4	1	−0.1	+18.3
	16.8	21.2	−4.3	2	−9.6	−11.5
perfluorocoronene	−3.4	6.7	−10.1	1	−2.9	+13.4
	15.4	17.4	−2.0	2	−13.3	−12.6

[a]The ring labels and the current strengths are also shown in Figure 7.

benzene to −16.5 ppm for hexafluorobenzene, suggesting that the degree of aromaticity increases with the number of fluorine substituents and that hexafluorobenzene is twice as aromatic as benzene. On the other hand, the NICS(0)$_{zz}$ values for the mono-, di-, and one of the trifluorinated benzenes are smaller than for benzene, whereas for the rest of the fluorinated benzenes the NICS$_{zz}$(0) values are larger than for benzene. Thus, according to the NICS$_{zz}$(0) values, the mono- and difluorinated benzenes are less aromatic than benzene whereas the tetra-, penta-, and hexafluorinated ones would be more aromatic than benzene. Different conclusions are reached depending on whether NICS(0) or NICS$_{zz}$(0) is used to assess the degree of aromaticity. However, the calculations of the ring-current strengths yield the opposite aromaticity trend, indicating that the NICS methods fail to provide the relative aromaticity of the fluorinated benzenes. NICS calculations using the modern and more sophisticated localized molecular orbital (LMO) method do not support the results obtained in traditional NICS calculations. LMO-NICS calculations suggest that benzene is as aromatic as perfluorinated benzene,[21] which does not agree with the results obtained in the current density calculations either. Thus, one should be prudent when interpreting the variety of NICS values as aromaticity indices.[28,61,65−67]

The reason for the failure of the NICS approach can be understood. Fluorine is a good σ acceptor, but it is also a good π donor. Due to its high electronegativity, fluorine withdraws electrons from benzene but only from the σ bonds. The carbon atoms gain, on the other hand, π electrons from fluorine. The redistribution of the electron charge due to fluorination is clearly seen in Figure 2. Donation of π electrons is weaker than the σ-acceptor contribution. In fluorinated benzenes, the carbons are somewhat electron depleted as compared to benzene. NICS values apparently depend mainly on the currents in the π-electron density above and below the ring, whereas the net ring current sustained along the edge of the molecule seems to contribute less to the NICS values at the ring center. GIMIC calculations describe the two effects correctly, whereas the NICS results do not correlate with the strength of the magnetically induced ring currents.

3.2. Linear Polyacenes. The current strengths are used for assessing the aromatic character and determining the current pathways. The signed modulus of the current densities is visualized in Figure 3. Current strengths confirm that the studied polyacenes are aromatic according to the ring-current criterion. Fluorination does not significantly change the aromatic character of the polyacenes. However, fluorine substitution decreases the current strengths by about 2.0−3.0 nA/T, suggesting that fluorination weakens the aromatic character of the polyacenes, which is in contrast to the conclusions drawn from the NICS values. The current strengths and NICS values of the linear polyacenes and their perfluorinated derivatives are given in Table 2, where the diatropic and paratropic contributions to the net current strength are reported for one of the C−C bonds of the individual rings. In the current-strength calculations, the integration plane is placed perpendicularly to the molecular plane, starting at the center of the investigated ring and crossing perpendicularly the C−C bond. The current strengths and current pathways of the polyacenes and the perfluorinated ones are shown in Figure 4. In the following, the current pathways and current strengths of the polyacenes are described in detail with the corresponding current strengths of the perfluorinated ones given in parentheses.

Current strengths for naphthalene reveal that a ring current of 12.7 (10.4) nA/T flows around the entire molecule, as also expected from symmetry arguments. The ring current flows on the outside along the edge of the molecule. The net current at the central bond vanishes, because the two contributions have the same strength and flow in opposite directions.

For anthracene, the central ring sustains a ring current of 3.4 (2.2) nA/T, whereas the strength of the ring current circling around the entire molecule is 12.1 (9.8) nA/T. The current pathway of tetracene consists of a weak current flow of 4.6 (3.3) nA/T around the central naphthalene moiety and a stronger one of 11.4 (9.4) nA/T around the whole molecule. No net current passes the central C−C bond due to symmetry.

Current pathway of pentacene can analogously be seen as a linear combination of three ring currents. One circles around the central benzene ring, one around the central anthracene moiety, and one around the entire pentacene. The calculated current strengths are 1.6 (1.2), 4.8 (3.6), and 10.5 (8.9) nA/T for rings 1, 2 and 3, respectively. Current strengths and current pathways of the perfluorinated polyacenes are given in Figure 4. The obtained current pathways and relative current strengths

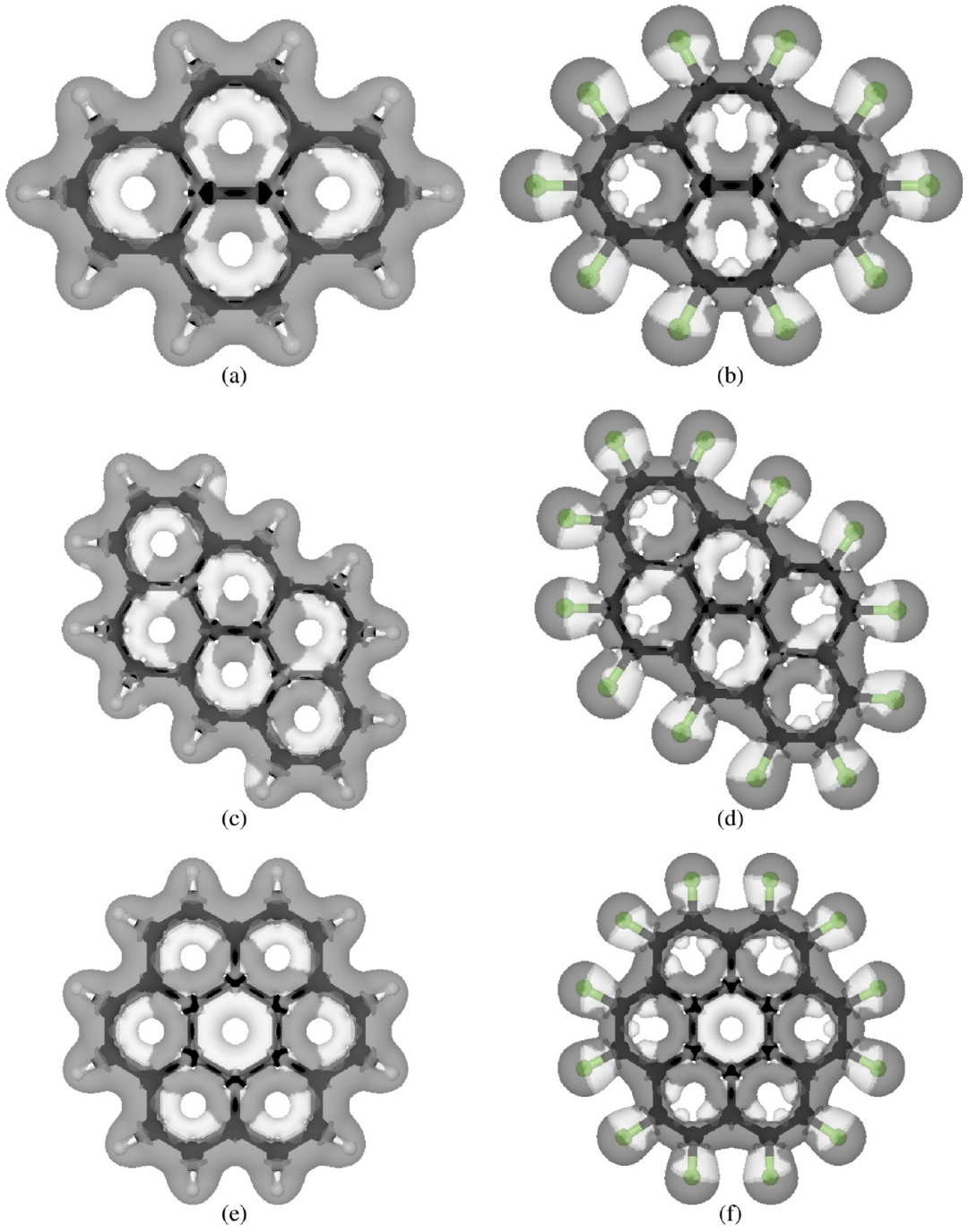

Figure 6. Signed modulus of the magnetically induced current densities calculated at the BP86/SVP level for (a) pyrene, (b) perfluoropyrene, (c) anthanthrene, (d) perfluoroanthanthrene, (e) coronene, (f) perfluorocoronene. The diatropic currents are gray and the paratropic ones are white.

for the unsubstituted polyacenes largely agree with those recently calculated at the ipsocentric coupled Hartree−Fock level by Fowler and Myrvold.[68] Steiner et al. also investigated larger polycyclic aromatic hydrocarbons using the same approach.[69]

The integrated current-strength profiles for pentacene and perfluoropentacene are given along the long molecular axis in Figure 5. The figure shows where the ring current passes the long molecular axis, starting (x = 0) in the middle of the central ring. The current-strength profiles for pentacene and perfluoropentacene are almost identical close to the molecular center, whereas significant differences appear at the ends of the molecule where the pentacene has stronger diatropic and paratropic currents than the perfluorinated one as for the benzene derivatives.

A closer look at the current strengths reveals that Kirchhoff's current law is not fulfilled. The current strengths calculated for different C−C bonds slightly differ even though they should be equal, implying that the divergence of the current density is not exactly zero everywhere.[23] The use of GIAOs removes gauge dependences of the current density but does not result in gauge invariance, which is the prerequisite of vanishing divergence. However, leakage is much smaller with GIAOs than when ordinary basis functions are employed. By employing basis sets of TZVP quality, current strengths are consistent within 0.1 nA/T. We use the SVP basis sets in this study because the shielding

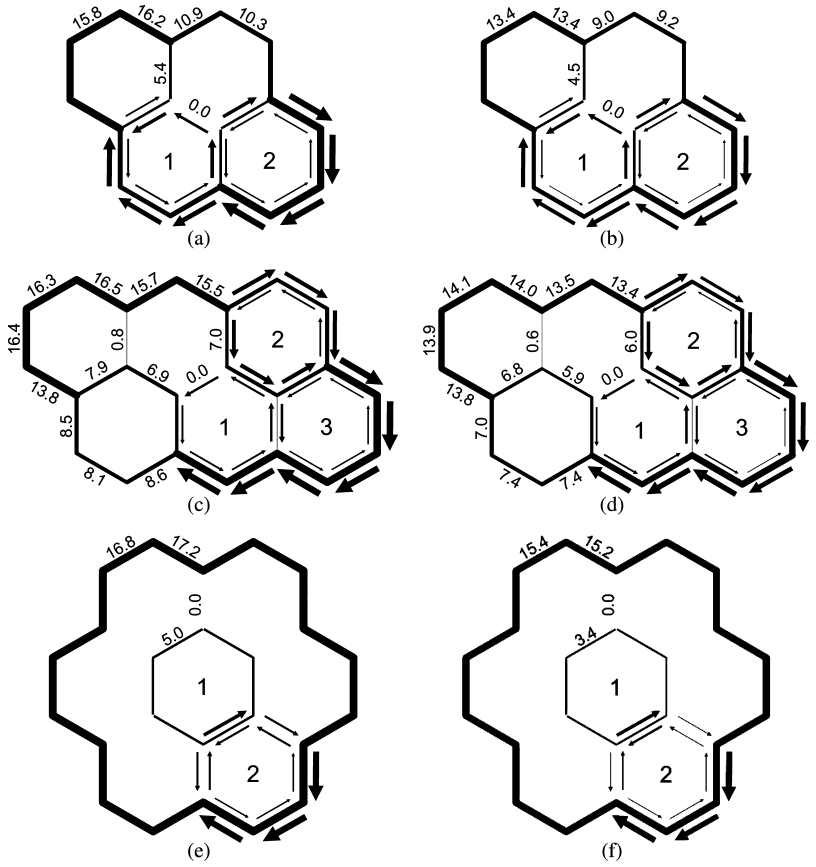

Figure 7. Integrated current strengths and current pathways for (a) pyrene, (c) anthanthrene, and (e) coronene (left) as well as their perfluorinated derivatives (right). Benzenoid rings are numbered taking the molecular symmetry into account.

calculations of the largest molecules are computationally expensive when the TZVP basis sets are employed. However, qualitatively the same results are obtained with the two basis sets.

The calculated NICS values indicate that all rings of the studied polyacenes are aromatic. For the perfluorinated polyacenes, the NICS(0) values of the individual rings are larger than for the unsubstituted ones, suggesting that fluorination strengthens the aromatic character. For the perfluorinated polyacenes, the NICS(0) values of the individual molecules are almost the same for all arene rings, whereas for the unsubstituted polyacenes they vary between −12 and −6 ppm. The central rings have larger NICS values than obtained for those at the ends of the linear polyacenes, suggesting that magnetically induced currents are stronger for rings closer to the molecular center. For the perfluorinated polyacenes, the NICS(0) values suggest that magnetically induced currents are more equally distributed over the molecules. $NICS_{zz}(0)$ values show the same trends as NICS(0) but with a broader distribution of the values.

3.3. Pyrene, Anthanthrene, and Coronene. Current calculations show that pyrene, anthanthrene, and coronene as well as the corresponding perfluorinated derivatives are aromatic according to the ring current criterion. The aromatic pathways for perfluoropyrene, anthanthrene, and coronene are also very similar to the unsubstituted ones. Therefore, the aromatic character of merely the unsubstituted molecules is discussed with the current strengths of the perfluorinated molecules given in parentheses. Calculated ring-current strengths are given in Table 3, and the signed modulus of the current densities is visualized in Figure 6.

The total current pathway in pyrene can be seen as a linear combination of an aromatic pathway around ring 2 and another one around the entire molecule. The strength of the current circling around ring 2 is 5.4 (4.5) nA/T, whereas a ring current of 10.9 (9.0) nA/T flows around the pyrene. Ring 1 cannot sustain any ring current of its own due to symmetry reasons. Current pathways are shown in Figure 7.

For anthanthrene, the main ring current flows around the whole molecule. Current pathway is split into two branches at ring 2. Current strength of the outer path is 8.1 (7.4) and 7.0 (6.0) nA/T for the inner route. Ring 3 sustains a very weak ring current of 0.8 (0.6) nA/T, whereas ring 1 does not sustain any ring current of its own due to the symmetry.

The current pathway of coronene consists of a net diatropic ring current around the edge of the molecule and a paratropic one circling around the innermost arene ring. The integrated current-strength function for coronene and perfluorocoronene showing the current that passes through a radial plane in the middle of the C−C bonds is shown in Figure 8. The integrated current flow is calculated with respect to the radial distance from the center of the inner arene ring. The figure shows that perfluorocoronene has weaker paratropic currents inside the molecule, especially inside the C−C bonds at the molecular edge. It also shows that the diatropic ring current along the outer periphery is stronger for coronene than for the perfluorinated one. The current strength of the edge current is 16.8 (15.4) nA/T, and the inner ring sustains a paratropic current of −5.0 (−3.4) nA/T. Thus, the perfluorinated molecules are somewhat less aromatic than the corresponding hydrocarbons.

dx.doi.org/10.1021/jp308121b | J. Phys. Chem. A 2012, 116, 10257−10268

The $NICS_{zz}(0)$ values given in Table 3 indicate that ring 1 is antiaromatic and ring 2 is aromatic, whereas the NICS(0) values suggest that ring 1 in coronene is weakly aromatic and ring 2 is at least as aromatic as benzene. Comparison of the calculated ring current strengths and pathways with the ones deduced from the NICS values shows that NICS calculations are not a very reliable means to assess the aromaticity of the individual rings. NICS(0) and $NICS_{zz}(0)$ values are reported for the individual rings in Table 3, but they will not be discussed for the larger polycyclic aromatic hydrocarbons and their perfluorinated derivatives.

3.4. Ovalene and Phenanthro-Ovalene. Integrated current strengths and calculated NICS values for ovalene and phenanthro-ovalene and the corresponding perfluorinated derivatives are given in Table 4. Comparison of the strength of the ring current circling around molecular rings with the NICS values of the individual arene rings shows that NICS values cannot be used to assess the aromaticity of the individual rings of polycyclic aromatic hydrocarbons and the perfluorinated analogs. The signed modulus of the magnetically induced current densities is visualized in Figure 9. Calculated current pathways and current strengths of ovalene and phenanthro-ovalene and their perfluorinated derivatives are summarized in Figure 10.

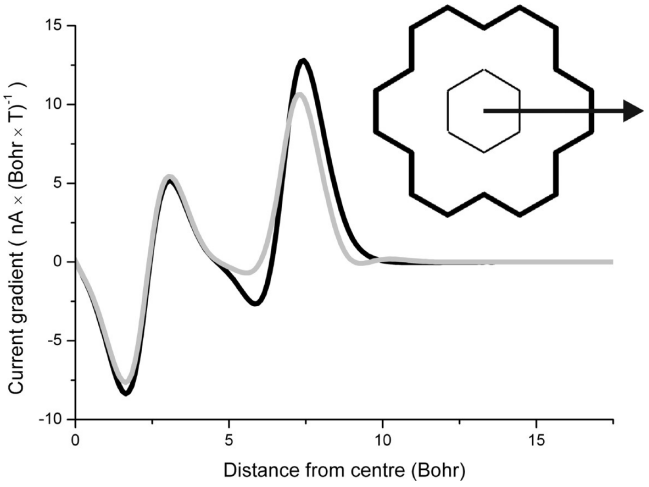

Figure 8. Integrated current strength as a function of the distance from the center of the molecule calculated for coronene (black) and perfluorocoronene (gray). Plane of the current profile is indicated by the arrow.

The current pathway of ovalene can be seen as the sum of three individual ring currents. The strength of the ring current circling around ring 1 is 5.5 (4.1) nA/T, a ring current of 4.6 (3.3) nA/T flows around ring 4, and finally a net diatropic current flow of 16.1 (15.0) nA/T circles around the entire ovalene molecule. Ring 2 does not sustain any ring current, but a very weak current of 0.6 (1.2) nA/T passes directly between rings 1 and 4. Ring 3 at the center cannot sustain any ring current due to the symmetry of the molecule. Values within parentheses refer to perfluoro-ovalene.

For phenanthro-ovalene, the current pathway can be decomposed into the following contributions. A paratropic current of −1.9 (−1.9) nA/T circles at the center of the molecule around ring 1. Ring 2 cannot sustain any ring current due to symmetry reasons. The main diatropic ring current flows along the outer edge of the entire molecule. The main ring current is split into two branches at ring 3. The current strength of the outer pathway is 14.1 (11.7) nA/T, and the strength of the inner route from ring 2 to ring 5 is 5.6 (6.0) nA/T. Ring 5 sustains a very weak ring current of 2.2 (1.3) nA/T. The net currents along the C−C bonds of ring 4 pass in different directions, implying that ring 4 cannot be considered to sustain any ring current of its own.

The integrated current-strength functions for ovalene and phenanthro-ovalene and the perfluorinated derivatives in Figure 11 show that current strengths in the interior of the fluorinated and unsubstituted molecules are practically identical, whereas along the outer edge the fluorinated derivatives have weaker paratropic currents inside the outermost C−C bond and a weaker diatropic along the molecular edge

Table 4. Comparison of Current Strengths (in nA/T) with the NICS(0) and $NICS(0)_{zz}$ Values (in ppm) Calculated for Ovalene and Phenanthro-Ovalene and the Perfluorinated Ones[a]

molecule	total	diatropic	paratropic	ring number	NICS(0)	$NICS(0)_{zz}$
ovalene	21.6	25.5	−3.9	1	−12.1	+18.2
	15.0	19.6	−4.6	2	−6.0	+0.8
	0	7.9	−7.9	3	−2.8	−10.6
	20.7	24.7	−4.0	4	−12.8	+21.2
perfluoro-ovalene	19.1	22.8	−3.6	1	−14.0	+13.8
	13.8	15.9	−2.1	2	−10.5	+14.8
	0	7.8	−7.8	3	−4.6	+11.0
	18.3	20.2	−1.9	4	−16.5	+12.0
phenanthro-ovalene	−1.9	6.7	−8.6	1	−3.1	−10.3
	21.6	25.5	−4.0	2	−10.7	+13.7
	14.1	18.8	−4.7	3	−4.2	−4.8
				4	−6.5	+0.4
	22.6	26.6	−3.9	5	−14.3	+25.7
perfluorophenanthro-ovalene	−1.9	6.8	−8.7	1	−3.5	+10.9
	18.3	22.0	−3.7	2	−12.2	+13.9
	11.7	14.1	−2.4	3	−7.8	+14.9
				4	−7.4	+10.9
	19.2	21.1	−1.9	5	−17.3	+11.9

[a]Ring labels and current strengths are also shown in Figure 4.

dx.doi.org/10.1021/jp308121b | J. Phys. Chem. A 2012, 116, 10257−10268

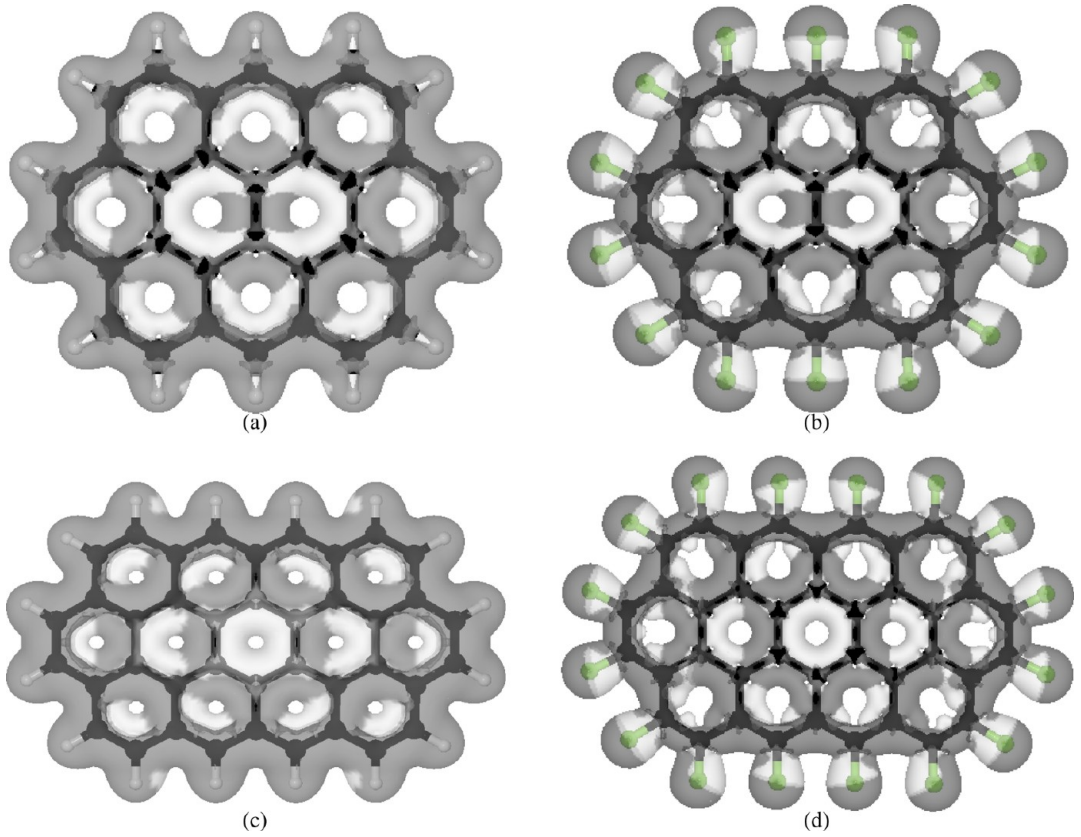

Figure 9. Signed modulus of the magnetically induced current densities calculated at the BP86/SVP level for (a) ovalene, (b) perfluoro-ovalene, (c) phenanthro-ovalene, and (d) perfluorophenanthro-ovalene. Diatropic currents are gray, and paratropic ones are white.

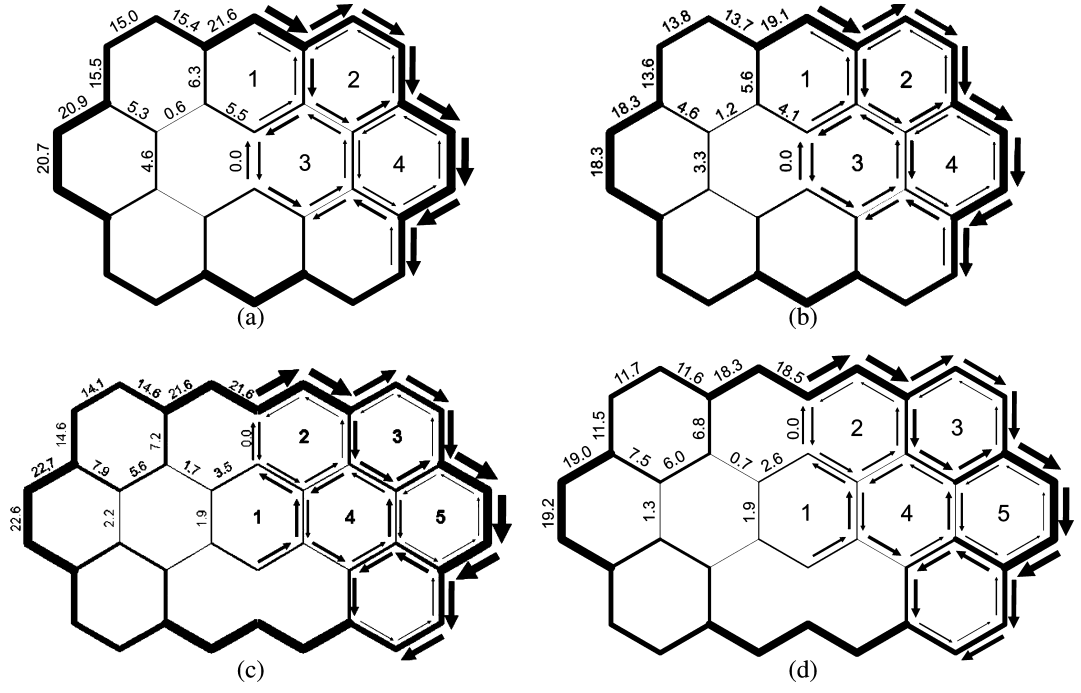

Figure 10. Integrated current strengths and current pathways for (a) ovalene, (b) perfluoro-ovalene, (c) phenanthro-ovalene, and (d) perfluorophenanthro-ovalene. Benzenoid rings are numbered taking the molecular symmetry into account.

than the unsubstituted ones. The smaller current strengths of the perfluorinated polycyclic aromatic hydrocarbons can be qualitatively understood. Substituted fluorines attract electrons, depleting electrons in the interior of the molecule. Because fewer electrons are available for electron delocalization and to transport the electrons, the currents are generally weaker than for the unsubstituted polycyclic aromatic hydrocarbons.

dx.doi.org/10.1021/jp308121b | J. Phys. Chem. A 2012, 116, 10257−10268

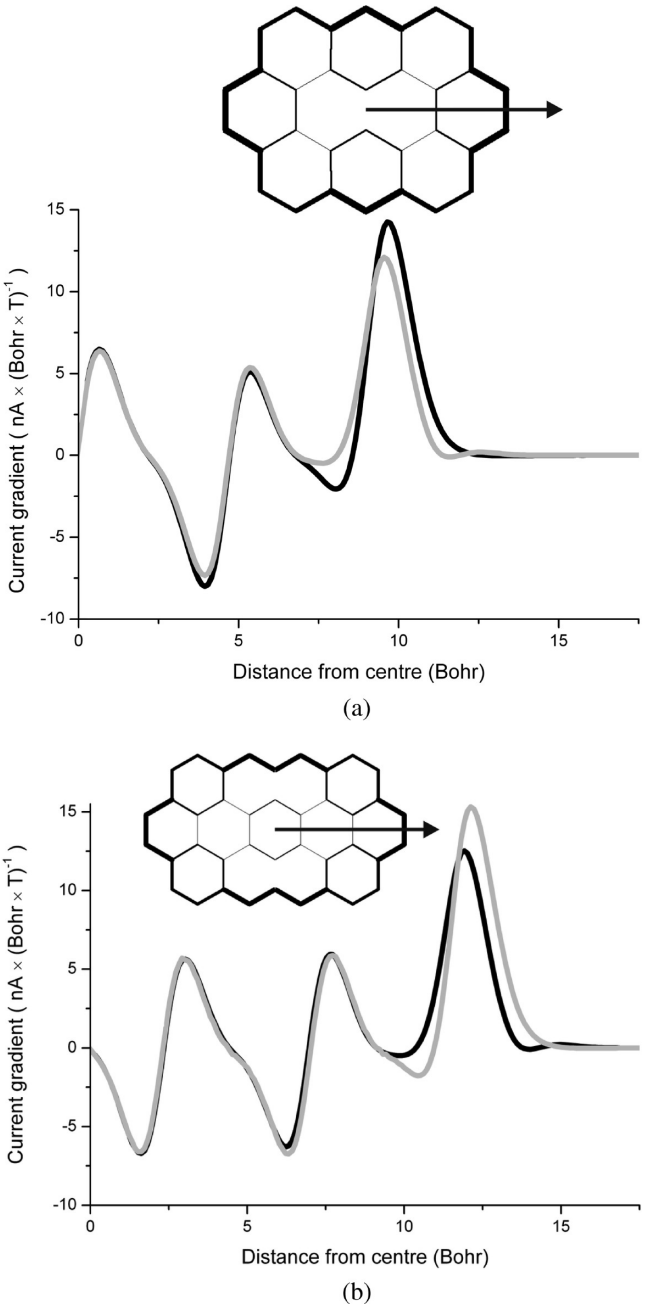

Figure 11. Integrated current strength as a function of the distance from the center of the molecule calculated for (a) ovalene and perfluoro-ovalene (gray) and (b) phenanthro-ovalene and perfluorophenanthro-ovalene (gray). Plane of the current profile is indicated by the arrow.

4. SUMMARY AND CONCLUSIONS

The magnetically induced current density for benzene and fluorinated benzene derivatives have been calculated using the gauge-including magnetically induced current method. A number of polycyclic aromatic hydrocarbons and the corresponding perfluorinated ones have also been investigated using GIMIC. Calculated current strengths passing selected C−C bonds are used for explicitly determining the current pathways in the molecules consisting of fused arene rings.

Benzene and all fluorinated benzene derivatives are aromatic according to the ring-current criterion. The degree of aromaticity of the benzene derivatives decreases with increasing number of fluorine substituents. Nucleus-independent chemical shifts suggest, on the other hand, that hexafluorobenzene is the most aromatic one among the studied benzene derivatives.

Current-strength calculations show that all molecules sustain strong ring currents flowing mainly around the entire molecule along the outer edge of the molecule. Current pathways of the perfluorinated molecules are the same as those for the corresponding hydrocarbons. Ring-current calculations show that the current strengths and thus the aromaticity generally decreases upon fluorination, especially along the C−C bonds at the edge of the molecules. Substituted fluorines attract electrons, leading to a depletion of electrons in the σ orbitals. For the larger polycyclic aromatic hydrocarbons, the currents in the interior of the molecule are only slightly weaker as compared to the unsubstituted ones. The change in the currents at the outermost carbons due to fluorine substitution is very similar for all investigated molecules.

For the fluorinated benzene derivatives, the failure of NICS can easily be understood. Fluorine is a strong σ acceptor but a weaker π donor, leading to electron depletion of the σ bonds, which is somewhat compensated by an increase in the π-electron density. NICS(0) values seem to be more sensitive to the currents in the π orbitals than in the σ orbitals, whereas the GIMIC calculations yield explicitly the total current passing through chemical bonds.

For the linear polyacenes, the NICS calculations yield erratic aromatic properties as compared to the GIMIC calculations. NICS calculations are apparently not a very reliable means to determine the degree of aromaticity in the individual rings of fused arene rings. For the polycyclic aromatic hydrocarbons as well as for the perfluorinated derivatives, the NICS values cannot provide sensitive information, because the magnetic shieldings in the center of the individual rings depend not only on the currents circling around the studied ring but also on the currents flowing around adjacent rings. Our results indicate that the NICS approach is not the right method of choice when assessing the local aromaticity of polycyclic aromatic hydrocarbons and derivatives thereof.

■ ASSOCIATED CONTENT

Ⓢ Supporting Information

Cartesian coordinates and nuclear magnetic shieldings of the studied molecules as well as thermochemical data for the series of fluorinated benzenes. This material is available free of charge via the Internet at http://pubs.acs.org.

■ AUTHOR INFORMATION

Corresponding Author

*E-mail: Mikko.Kaipio@helsinki.fi; Michael.Patzschke@helsinki.fi; Heike.Fliegl@kjemi.uio.no; fabio@che.tohoku.ac.jp; Dage.Sundholm@helsinki.fi.

Notes

The authors declare no competing financial interest.

■ ACKNOWLEDGMENTS

This research was supported by the Academy of Finland through its Centers of Excellence Programme 2006−2011. We thank the Graduate School of Engineering of Tohoku University and Magnus Ehrnrooth foundation for financial support. CSC, the Finnish IT Center for Science, is acknowledged for computer time. H.F. thanks the Norwegian Research Council for support through the CeO Centre for Theoretical and Computational Chemistry (Grant No. 179568/V30).

REFERENCES

(1) Pauling, L. *The Nature of the Chemical Bond*, 3rd ed.; Cornell University Press, 1960.
(2) Bent, H. A. *Chem. Rev.* **1961**, *61*, 275−311.
(3) Spieseke, H.; Schneider, W. G. *J. Chem. Phys.* **1961**, *35*, 722−730.
(4) Clasen, C. A.; Good, M. L. *Inorg. Chem.* **1970**, *9*, 817−820.
(5) Smart, B. E. *J. Fluorine Chem.* **2001**, *109*, 3−11.
(6) Porhiel, E.; Toupet, L.; Leroy, J.; Bondon, A. *Tetrahedron Lett.* **2002**, *43*, 8293−8296.
(7) Lai, S.-W.; Hou, Y.-J.; Che, C.-M.; Pang, H.-L.; Wong, K.-Z.; Chang, C. K.; Zhu, N. *Inorg. Chem.* **2004**, *43*, 3724−3732.
(8) Hagmann, W. K. *J. Med. Chem.* **2008**, *51*, 4359−4369.
(9) Qiu, X. L.; Meng, W. D.; Qing, F. L. *Tetrahedron* **2004**, *60*, 6711−6745.
(10) Liu, H.-Y.; Lai, T.-S.; Yeung, L.-L.; Chang, C. K. *Org. Lett.* **2003**, *5*, 617−620.
(11) Houde, M.; De Silva, A. O.; Muir, D. C. G.; Letcher, R. J. *Environ. Sci. Technol.* **2011**, *45*, 7962−7973.
(12) Feng, X.; Li, Q.; Gu, J.; Cotton, F. A.; Xie, Y.; Schaefer, H. F., III *J. Phys. Chem. A* **2009**, *113*, 887−894.
(13) Lemal, D. M. *J. Org. Chem.* **2009**, *74*, 2413−2416.
(14) Entani, S.; Kaij, T.; Ikeda, S.; Mori, T.; Kikuzawa, Y.; Takeuchi, H.; Saiki, K. *J. Phys. Chem. C* **2009**, *113*, 6202−6207.
(15) Sakamoto, Y.; Suzuki, T.; Kobayashi, M.; Gao, Y.; Fukai, Y.; Inoue, T.; Sato, F.; Tokito, S. *J. Am. Chem. Soc.* **2004**, *126*, 8138−8140.
(16) Alkorta, I.; Rozas, I.; Elguero, J. *J. Fluorine Chem.* **2000**, *101*, 233−238.
(17) Pichierri, F. *Chem. Phys. Lett.* **2003**, *376*, 781−787.
(18) Pichierri, F. *J. Mol. Struct. (THEOCHEM)* **2008**, *870*, 36−42.
(19) Fliegl, H.; Lehtonen, O.; Sundholm, D.; Kaila, V. R. I. *Phys. Chem. Chem. Phys.* **2011**, *13*, 434−437.
(20) Okazaki, T.; Laali, K. K. *Org. Biomol. Chem.* **2006**, *4*, 3085−3095.
(21) Wu, J. I.; Pühlhofer, F. G.; von Ragué Schleyer, P.; Puchta, R.; Kiran, B.; Mauksch, M.; van Eikema Hommes, N. J. R.; Alkorta, I.; Elguero, J. *J. Phys. Chem. A* **2009**, *113*, 6789−6794.
(22) von Ragué Schleyer, P.; Manoharan, M.; Wang, Z.-X.; Kiran, B.; Jiao, H.; Puchta, R.; van Eikema Hommes, N. J. R. *Org. Lett.* **2001**, *3*, 2465−2468.
(23) Jusélius, J.; Sundholm, D.; Gauss, J. *J. Chem. Phys.* **2004**, *121*, 3952−3963.
(24) Taubert, S.; Sundholm, D.; Jusélius, J. *J. Chem. Phys.* **2011**, *134* (054123), 1−12.
(25) Fliegl, H.; Sundholm, D.; Taubert, S.; Jusélius, J.; Klopper, W. *J. Phys. Chem. A* **2009**, *113*, 8668−8676.
(26) Lin, Y. C.; Jusélius, J.; Sundholm, D.; Gauss, J. *J. Chem. Phys.* **2005**, *122* (214308), 1−9.
(27) Lin, Y. C.; Sundholm, D.; Jusélius, J.; Cui, L. F.; Li, X.; Zhai, H. J.; Wang, L. S. *J. Phys. Chem. A* **2006**, *110*, 4244−4250.
(28) Lin, Y. C.; Sundholm, D.; Jusélius, J. *J. Chem. Theory Comput.* **2006**, *2*, 761−764.
(29) Fliegl, H.; Lehtonen, O.; Patzschke, M.; Sundholm, D.; Lin, Y. C. *Theor. Chem. Acc.* **2011**, *129*, 701−713.
(30) Johansson, M. P.; Jusélius, J.; Sundholm, D. *Angew. Chem., Int. Ed.* **2005**, *44*, 1843−1846.
(31) Jusélius, J.; Sundholm, D. *Phys. Chem. Chem. Phys.* **2008**, *10*, 6630−6634.
(32) Taubert, S.; Jusélius, J.; Sundholm, D.; Klopper, W.; Fliegl, H. *J. Phys. Chem. A* **2008**, *112*, 13584−13592.
(33) Taubert, S.; Sundholm, D.; Pichierri, F. *J. Org. Chem.* **2009**, *74*, 6495−6502.
(34) Taubert, S.; Sundholm, D.; Pichierri, F. *J. Org. Chem.* **2010**, *75*, 5867−5874.
(35) Fliegl, H.; Sundholm, D.; Taubert, S.; Pichierri, F. *J. Phys. Chem. A* **2010**, *114*, 7153−7161.
(36) Taubert, S.; Kaila, V. R. I.; Sundholm, D. *Int. J. Quantum Chem.* **2011**, *111*, 848−857.
(37) Fliegl, H.; Sundholm, D.; Pichierri, F. *Phys. Chem. Chem. Phys.* **2011**, *13*, 20659−20665.
(38) Fliegl, H.; Sundholm, D. *J. Org. Chem.* **2012**, *77*, 3408−3414.
(39) Fliegl, H.; Taubert, S.; Lehtonen, O.; Sundholm, D. *Phys. Chem. Chem. Phys.* **2011**, *13*, 20500−20518.
(40) Ahlrichs, R.; Bär, M.; Häser, M.; Horn, H.; Kölmel, C. *Chem. Phys. Lett.* **1989**, *162*, 165−169.
(41) Becke, A. D. *J. Chem. Phys.* **1993**, *98*, 5648−5652.
(42) Lee, C.; Yang, W.; Parr, R. G. *Phys. Rev. B* **1988**, *37*, 785−789.
(43) Weigend, F.; Ahlrichs, R. *Phys. Chem. Chem. Phys.* **2005**, *7*, 3297−3305.
(44) Schäfer, A.; Horn, H.; Ahlrichs, R. *J. Chem. Phys.* **1992**, *97*, 2571−2577.
(45) Deglmann, P.; Furche, F. *Chem. Phys. Lett.* **2002**, *362*, 511−518.
(46) Vosko, S. H.; Wilk, L.; Nusair, M. *Can. J. Phys* **1980**, *58*, 1200−1211.
(47) Perdew, J. P. *Phys. Rev. B* **1986**, *33*, 8822−8824.
(48) Becke, A. D. *Phys. Rev. A* **1988**, *38*, 3098−3100.
(49) Wolinski, K.; Hinton, J. F.; Pulay, P. *J. Am. Chem. Soc.* **1990**, *112*, 8251−8260.
(50) Häser, M.; Ahlrichs, R.; Baron, H. P.; Weis, P.; Horn, H. *Theor. Chim. Acta* **1992**, *83*, 455−470.
(51) Kollwitz, M.; Häser, M.; Gauss, J. *J. Chem. Phys.* **1998**, *108*, 8295−8301.
(52) London, F. *J. Phys. Radium* **1937**, *8*, 397−409.
(53) Hameka, H. F. *Mol. Phys.* **1958**, *1*, 203−215.
(54) Ditchfield, R. *Mol. Phys.* **1974**, *27*, 789−807.
(55) *Jmol: an open-source Java viewer for chemical structures in 3D*; http://www.jmol.org.
(56) http://www.gnuplot.info/.
(57) *Gimp: GNU Image Manipulation Program*; http://www.gimp.org.
(58) *ChemDraw ULTRA 12.0 SUITE*; Perkin Elmer; http://www.cambridgesoft.com.
(59) von Ragué Schleyer, P.; Maerker, C.; Dransfeld, A.; Jiao, H.; van Eikema Hommes, N. J. R. *J. Am. Chem. Soc.* **1996**, *118*, 6317−6318.
(60) Fallah-Bagher-Shaidaei, H.; Wannere, C. S.; Corminboeuf, C.; Puchta, R.; von Ragué Schleyer, P. *Org. Lett.* **2006**, *8*, 863−866.
(61) Lazzeretti, P. *Phys. Chem. Chem. Phys.* **2004**, *6*, 217−223.
(62) Brundle, C. R.; Robin, M. B.; Kuebler, N. A. *J. Am. Chem. Soc.* **1972**, *94*, 1466−1475.
(63) Laaksonen, L. *J. Mol. Graph.* **1992**, *10*, 33−34.
(64) Bergman, D. L.; Laaksonen, L.; Laaksonen, A. *J. Mol. Graph. Model.* **1997**, *15*, 301−306.
(65) Jusélius, J.; Sundholm, D. *Phys. Chem. Chem. Phys.* **1999**, *1*, 3429−3435.
(66) Lazzeretti, P. *Prog. Nucl. Magn. Reson. Spectrosc.* **2000**, *36*, 1−88.
(67) Islas, R.; Martínez-Guajardo, G.; Jiménez-Halla, J. O. C.; Solá, M.; Merino, G. *J. Chem. Theory Comput.* **2010**, *6*, 1131−1135.
(68) Fowler, P. W.; Myrvold, W. *J. Phys. Chem. A* **2011**, *115*, 13191−13200.
(69) Steiner, E.; Fowler, P. W.; Soncini, A.; Jenneskens, L. W. *Faraday Discuss.* **2007**, *135*, 309−323.